Journal of Maps

ISSN: (Print) (Online) Journal homepage: www.tandfonline.com/journals/tjom20

A GIS-based multiscale mapping framework to assess and visualize complex and polygenetic geomorphic systems – A novel 'Geomorphic Entities' approach

Manuel La Licata, Alberto Bosino, Mattia De Amicis, Andrea Terret & Michael Maerker

To cite this article: Manuel La Licata, Alberto Bosino, Mattia De Amicis, Andrea Terret & Michael Maerker (2025) A GIS-based multiscale mapping framework to assess and visualize complex and polygenetic geomorphic systems – A novel 'Geomorphic Entities' approach, Journal of Maps, 21:1, 2437256, DOI: 10.1080/17445647.2024.2437256

To link to this article: https://doi.org/10.1080/17445647.2024.2437256

JOURNAL OF MAPS
2025, VOL. 21, NO. 1, 2437256
https://doi.org/10.1080/17445647.2024.2437256

A GIS-based multiscale mapping framework to assess and visualize complex and polygenetic geomorphic systems – A novel 'Geomorphic Entities' approach

Manuel La Licata [a,b,c], Alberto Bosino [d], Mattia De Amicis[d], Andrea Terret[e] and Michael Maerker[a,b,c]

[a]Department of Earth and Environmental Sciences, University of Pavia, Pavia, Italy; [b]Institute of Geosciences and Earth Resources, National Research Council of Italy, Pavia, Italy; [c]Working Group on Soil Erosion and Feedbacks, Leibniz Centre for Agricultural Landscape Research (ZALF), Müncheberg, Germany; [d]Department of Earth and Environmental Sciences, University of Milano-Bicocca, Milano, Italy; [e]Consorzio di Bonifica di Piacenza, Piacenza, Italy

ABSTRACT

This paper presents a novel GIS-based methodological framework for multiscale digital mapping and database implementation in sediment dynamics assessments. It relies on the concept of 'Geomorphic Entities' (GEs), which are polygon objects representing complex, polygenetic geomorphic systems. GEs allow mapping 'focal landforms' as elementary mapping units, while the database stores hierarchical information on sediment sources/sinks classification, process composition, activity, and morphodynamics. We tested this approach in the upper Val d'Arda (N-Apennines, Italy), integrating pre-existing geomorphological datasets with field assessments, photointerpretation, terrain analysis, semi-automated landform classification, and manual digital mapping to produce an Inventory Map of GEs. The primary result is a WebGIS application, allowing end-users to consult and query geospatial data and associated attributes interactively. By combining geomorphological and GIS expertise, this framework addresses the limitations of classical symbol-oriented maps, supporting scientific and applied purposes. It complements traditional mapping methods by structuring complex geomorphological data for use in integrated modelling procedures.

ARTICLE HISTORY
Received 31 March 2024
Revised 18 November 2024
Accepted 27 November 2024

KEYWORDS
Geomorphological mapping; general framework; geomorphic entities; inventory map; sediment sources; WebGIS

1. Introduction

Over the last decades, geomorphological studies have been widely applied to assist decision-makers in effectively managing soil erosion and sediment yield at the watershed scale (Renschler & Harbor, 2002). In this framework, multiscale geomorphological mapping plays a crucial role in understanding earth surface processes and the related morphodynamics (Bishop et al., 2012). Multiscale geomorphological mapping has proven to be a useful tool for land management, especially in the field of geohazard evaluation and risk mitigation (Dramis et al., 2011).

GIS-based digital mapping allows to produce maps which can be updated, integrated, and implemented in further steps (Bufalini et al., 2021). This approach provides a digital collection of different data layers and/or objects (Gustavsson et al., 2008), including information on the terrain surface derived from Digital Terrain Models (DTMs) (Maerker et al., 2019; Minár et al., 2024). Moreover, it can include both field-based mapping approaches and (semi-)automatic DTM-based landform classification and mapping (e.g. Bufalini et al., 2021; La Licata et al., 2023).

Land surface features can be represented on a digital map using various types of data, such as raster or vector data (*i.e.* point, lines, or polygons), which can be combined with attribute data describing their characteristics (Seijmonsbergen, 2013). The database typically collects information on the morphology, morphogenesis, morphometry, hydrography, lithology, structure, and age of landforms as mutually independent factors (Gustavsson et al., 2006). Moreover, digital maps allow for rapid handling and elaboration of thematic layers, the achievement of numerical analysis, and automatic extraction of the information (Dramis et al., 2011). Furthermore, analyzing the relationship between geomorphic process distribution and environmental parameters leads to a better understanding of trigger mechanisms, as well as of the behaviour of geomorphic systems over time (Bartelletti et al., 2017).

The integration of geomorphological mapping and GIS processing is often employed to assess sediment

CONTACT Manuel Licata manuel.lalicata01@universitadipavia.it Department of Earth and Environmental Sciences, University of Pavia, Via Ferrata 1, Pavia, 27100, Italy; Institute of Geosciences and Earth Resources, National Research Council of Italy, Via Ferrata 1, Pavia, 27100, Italy; Working Group on Soil Erosion and Feedbacks, Leibniz Centre for Agricultural Landscape Research (ZALF), Eberswalder Straße 84, 15374 - Müncheberg, Germany
Supplemental map for this article is available online at https://doi.org/10.1080/17445647.2024.2437256.

dynamics (*e.g.* Maerker et al., 2001; Theler et al., 2008, 2010; Bollati et al., 2024). Basically, the assessment of spatial distribution and geometric characteristics of sediment-related geomorphic features is generally a key prerequisite for assessing process-based susceptibilities and specific sediment transport dynamics (Bosino et al., 2022; Cho et al., 2023). Based on this assessment, it is possible to design effective management strategies in order to achieve meaningful reductions in sediment-related threats (Najafi et al., 2021; Sadeghi et al., 2014). However, the identification of hotspots of sediment dynamics to which the necessary attention must be directed should consider the variety of processes acting at the different spatio-temporal scales (La Licata et al., 2024). Thus, mapping the complexity of sediment dynamics (Gao et al., 2019) might be quite difficult in highly active complex geomorphic systems characterized by multiple and/or overlaying processes, and affected also by interacting anthropic activities (La Licata et al., 2023).

Despite the fact that geospatial technologies have greatly improved geomorphological mapping in the last decades (Bishop & Shroder, 2004; James et al., 2012), issues related to space–time variation in the context of processes and surface-object evolution still remain (Gustavsson et al., 2006). From this viewpoint, dynamic representations of forms and processes are quite limited using traditional 'static' cartographic approaches or by using ambiguous and/or not standardized terminology related to scale and spatial entities (Bishop et al., 2012). According to Dramis et al. (2011), multiscale mapping frameworks, coherently managed with a GIS and applicable for cross-disciplinary analysis, should be based on correctly bounded geometric elements/entities implementable and manageable in a database (object-oriented maps) instead of using specific genetic- and scale-dependent symbols (symbol-oriented maps) (e.g. Buter et al., 2020). In this regard, object-oriented mapping schemes can be adapted to meet specific needs for managing complex geomorphological data through hierarchical, scalable classifications, allowing for detailed analysis and flexible adaptation to different scales and applications (Magliuolo & Valente, 2020), as well as to adhere to data transfer standards and to facilitate interoperability across different computer systems (Dramis et al., 2011).

Moreover, some studies pointed out that traditional landform-oriented geomorphological maps are not fully satisfactory for evidencing the importance of sediment storage systems and their potential contribution to sediment dynamics, as the represented landforms may change very quickly over a short spatial and temporal scale in dynamic environments (Theler & Reynard, 2008). In this regard, more dynamic approaches that integrate both process-oriented and genetic-based geomorphological mapping for semi-quantitative assessments of sediment cascades have been proposed (e.g. Theler et al., 2010). However, processes like erosion, sediment transport, and deposition vary significantly over time and space, making it challenging to precisely define their boundaries and spatial extent on a map. Therefore, process-oriented maps may require extensive field-based and remote sensing data, frequently updated information, and continuous monitoring to accurately assess morphodynamics.

In this context, La Licata et al. (2024) employed a novel GIS-based multiscale mapping approach for assessing and characterizing sediment sources and sinks within the HOTSED semi-quantitative modelling framework. It integrates both landform- and process-oriented mapping schemes to assess spatially delimited polygenetic geomorphic systems, characterized by a scale-dependent and morphogenetic-based hierarchical process composition. The elementary mapping unit essentially corresponds to the 'focal landform' (landform unit), as proposed by Campobasso et al. (2023), which is represented on the map using polygon entities (i.e. Geomorphic Entities). Unlike 'full-coverage' mapping schemes that characterize the entire topographic surface in terms of associated landforms and deposits using a hierarchical-nested approach (e.g. Bufalini et al., 2021; Campobasso et al., 2023; Dramis et al., 2011), the approach adopted by La Licata et al. (2024) focuses exclusively on mapping sediment-related landforms (erosion or deposition) related to the primary/dominant morphogenetic processes at a defined focal scale. Secondary processes associated with primary morphogenesis, as well as subordinate processes linked to a subsequent/overlaying morphogenetic system, both of which act as secondary contributors to sediment dynamics on the same mapped landform, are surveyed at a greater scale and integrated as attributes in the database. Additionally, information related to morphodynamics, such as present activity and evolutionary trends of geomorphic systems, is assessed through multi-temporal image series analysis and incorporated into the database. Thus, the novelty of this approach lies in its ability to efficiently manage complex, dynamic, multiscale geomorphological spatial data using single, spatially defined, and overlapping polygonal geomorphic entities, facilitating the integration of these data into modelling procedures.

Building upon this previous work, in this paper we formalize and further elaborate this multiscale mapping framework (La Licata et al., 2024). Specifically, we aim to provide a more rigorous and schematic description of the general methodological framework, focusing on the underlying concepts and definitions, to enhance its applicability and reproducibility. Since this approach can be used complementarily to traditional cartographic methods, we compare it with classical symbol-oriented maps to illustrate the contexts in which our method can be applied and how

its use may be beneficial. The methodology illustrated herein was applied to the upper Val d'Arda (Northern Apennines, Italy). We selected this watershed since it is an open laboratory for studying different processes that are part of complex and polygenetic geomorphic systems. Hence, the area is suitable to emphasize the structure of the methodological workflow. Finally, we implemented a WebGIS application to support the dissemination and integrated visualization of spatial information (Veenendaal et al., 2017), as well as to facilitate the applicability of this approach.

2. Study area

The upper Val d'Arda is located in the Northern Apennines, Emilia-Romagna region, Italy. The study area covers the watershed upstream of the Mignano reservoir, which is an artificial basin exploited for irrigation purposes. It stretches SW-NE for ~14 km and extends for ~ 88 km^2. The altitudinal range varies from 285 to 1,356 m a.s.l (Mt. Menegosa).

The geological context is related to the External Ligurian Domain (Marroni et al., 2001). According to Servizio Geologico d'Italia (1999), the study area is characterized by lithological units dating from the Upper Cretaceous to the Paleocene-Eocene periods, which can be summarized as follows: (i) calcareous and silicoclastic marly turbidites (*Mt. Cassio Flysch*); (ii) varicoloured clays with intercalated layers of turbiditic sandstones (*Cassio Varicoloured Shales*); (iii) turbidites made up of lithoarenites and silty marly pelites (*Scabiazza Sandstones*); (iv) turbidites made up of calcarenitic marly limestones and marls (*Bettola Flysch*); (v) argillites with intercalations of turbiditic arenites, calcareous-marly turbidites, or sedimentary and ophiolitic breccias (*Guselli Argillites*); (vi) arenaceous-pelitic and calcareous-marly turbidites (*Farini d'Olmo Flysch*); (vii) sedimentary mélanges associated with matrix- to clast supported polygenetic breccias and ophiolitic sandstones (*Pietra Parcellara Complex*) (Martini & Zanzucchi, 2000).

The upper Val d'Arda is of particular interest concerning land degradation processes. Its heterogeneity in terms of lithological and morphological features promotes a great variety of complex and polygenetic geomorphic systems (La Licata et al., 2023). Landslides are extensively distributed in the study area. They contribute to the sediment delivery with multiple and interacting processes showing high variability of magnitudes and frequencies (Figure 1a). Other processes such as fluvial and rill-interrill erosion act as sediment sources, significantly contributing to the sediment yield (Figuere 1b, c). Badlands are mostly limited in extent by lithological constraints (i.e. varicoloured clays; Figure 1d), where piping and tunnelling have a significant role in their development. These processes are spatially and temporally combined and are responsible for the sediment discharge into the drainage system. Moreover, the Mignano reservoir is intensely affected by reservoir siltation (Patro et al., 2022) (Figure 1e). Nonetheless, only a fraction of the sediments eroded from hillslopes is deposited in the reservoir, while the remaining part is stored within the watershed in depositional landforms such as large landslide bodies as well as slope and alluvial deposits (Figure 1f, g, h). However, the latter are frequently affected by subsequent and overimposed erosion processes that contribute to the remobilization and transport of sediments.

The study area has a humid warm temperate climate, with very hot-warm summers and with very low or without water deficit (Cfa and Cfb, Köppen-Geiger climate types; Kottek et al., 2006). The mean annual air temperature is 11.4 °C at 342 m a.s.l. and 9.7 °C at 1,077 m a.s.l. The mean annual rainfall at lower and higher altitudes is respectively 930 mm and 1,155 mm, with a bimodal trend with maxima in spring and autumn (La Licata et al., 2023).

Soils develop under biochemical alteration and incipient or complete decarbonation. Soils with strong profile differentiation, complete decarbonation, and mild acidification (*Eutric Cambisols* and *Dystric Cambisols*) are present on more stable slopes, both on calcaric and ophiolitic parent material. Conversely, partially decarbonated soils (*Calcaric Cambisols*) are dominant on marly-calcareous and arenaceous-pelitic parent material, particularly in areas affected by mass movements and soil erosion. Less developed soils (*Calcaric Regosols*) are present on convex, steep, and erosive slopes with scarce vegetation cover (IUSS Working Group, 2015; Regione Emilia-Romagna, 1994).

The study area is characterized by the widespread presence of arable lands (~1,560 ha). Forest vegetation is mostly composed of oak, hornbeam, and chestnut woods at lower altitudes and beech woods at higher ones. Deciduous, coniferous and mixed coppice and high forests are widespread. Orchards and vineyards are also present (Regione Emilia-Romagna, 1994).

3. Materials and methods

3.1. General mapping framework: concepts and definitions

The mapping process is based on the identification of geomorphic systems characterized by a scale-dependent and morphogenetic-based hierarchical process composition (Figure 2). These geomorphic systems are geometrically represented and digitized in a GIS environment by using polygon objects, herein called 'Geomorphic Entities' (GEs) (Figure 2). In the present work, GEs are defined by a set of criteria. In particular:

- They are based on *focal landforms* (or landform units) uniquely delimited in space (*sensu*

Figure 1. Geomorphic processes and related landforms of the upper Val d'Arda: (a) mudflow with pine colonization; (b) river-related slope erosion at the landslide toe; (c) rill-interrill erosion on arable land; (d) rill erosion features on a badland set on varicoloured clays; (e) sedimentation within Mignano reservoir; (f) debris cones at the base of an ophiolitic outcrop; (g) alluvial plain of the Arda river with evidence of human alteration due to excavation; (h) toe of a complex dormant kilometre-size landslide body.

Campobasso et al., 2023; i.e. characterized by a specific distinctive configuration of the dominant morphogenetic processes that generated them);

- They involve one or multiple overlapping processes (i.e. levels of processes) occurring over various spatial scales;
- They involve processes potentially interacting with watershed hydrology and external drivers over various temporal scales;
- Depending on the process composition, they contribute to sediment accumulation or sediment export or a combination of both.

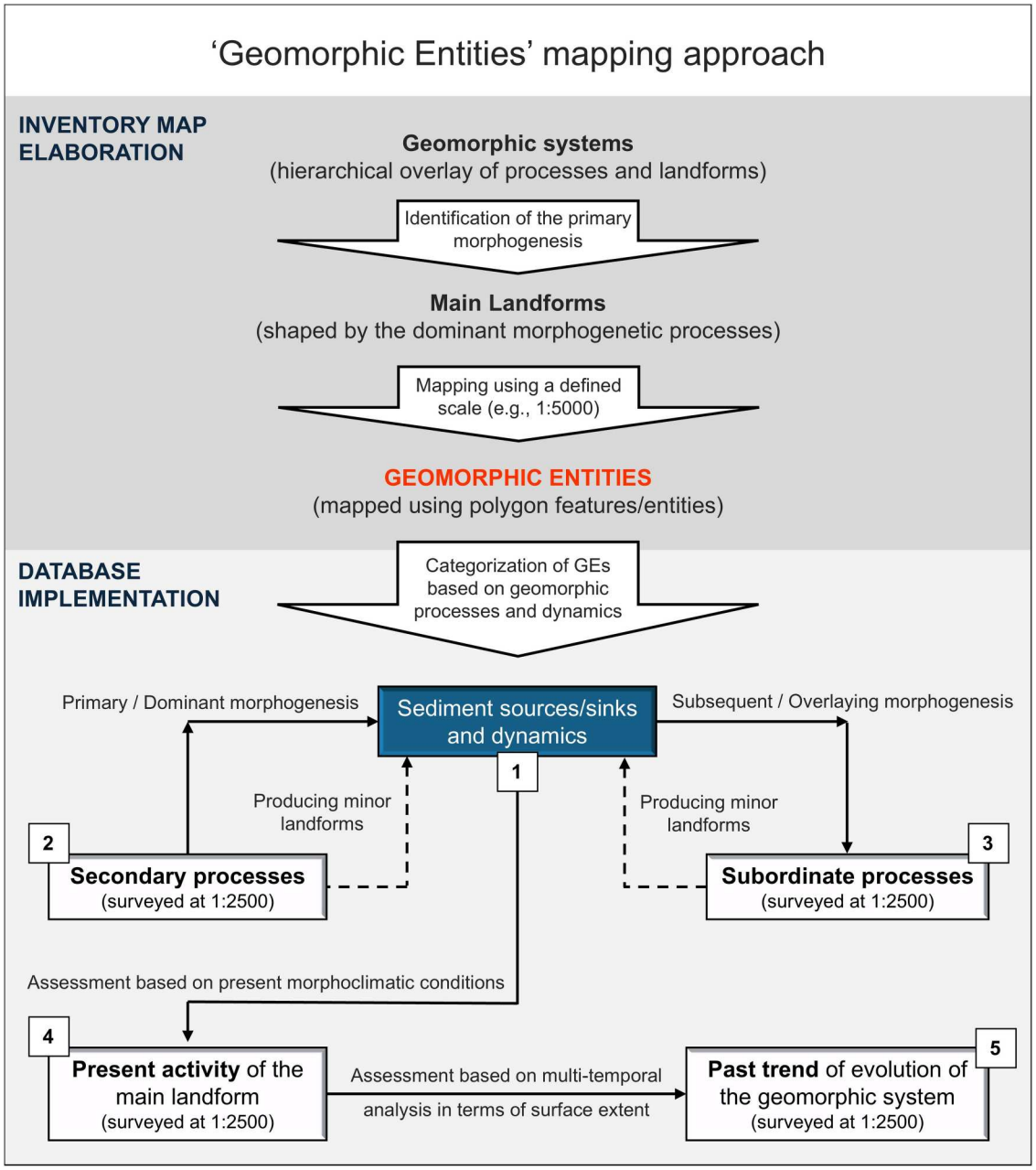

Figure 2. Flowchart of the new 'Geomorphic Entities' mapping approach designated in this study. The database variables/attributes (1) *Sediment sources/sinks and dynamics*, (2) *Secondary processes*, (3) *Subordinate processes*, (4) *Present activity of the main landform*, and (5) *Past trend of evolution of the geomorphic system* are defined in Table 1. The variable n. 1 is used as the reference variable. Modified after La Licata et al. (2024).

Considering the polygenetic nature of GEs, the initial mapping focuses on identifying the main (focal) landforms shaped by dominant processes (in terms of occurrence and extent) associated with the primary morphogenesis (Panizza, 1972), while setting an appropriate scale (e.g. 1:5,000). Then, the entire set of GEs is implemented within a GIS-based Inventory Map (IM) (Figure 2), conveying information on their location and spatial distribution. Particularly, the GEs dataset can be implemented through a unique vector layer or split into multiple layers depending on data structure and organization, practical purposes, and/or specific applications. Generally, GEs grouping can be achieved following classical geomorphological criteria (e.g. main categories of morphogenetic processes, erosion and deposition dynamics, litho-structural control on processes).

Subsequently, a corresponding database (i.e. attribute table) is developed in order to collect information useful for characterizing the GEs. A hierarchically organized structure is implemented to account for complex and polygenetic systems. Specifically, each GE is characterized and categorized according to the attributes defined in Table 1 (i.e. 1–5; Figure 2).

The attribute *Sediment sources/sinks and dynamics* is used as the reference variable as it is essentially a more specific categorization of the main landforms mapped as GEs (Figure 2). Moreover, the categorization of *Secondary processes* and *Subordinate processes* essentially depends on their relative small-scale and

Table 1. Definition of the attributes considered for the implementation of the Inventory Map database (Figure 2). The definition of the *Present activity of the main landform* is based on Campobasso et al. (2021).

Variable	Attribute	Definition
1	Sediment sources/sinks and dynamics	Specific morphological and geomorphic characteristics through which landforms mapped as GEs can be uniquely classified as sediment sources/sinks, based on the dominant morphogenetic process and sediment dynamic.
2	Secondary processes	Processes related to the primary morphogenesis, acting as secondary contributors. When present, these processes are minor compared to the dominant ones but still affect the overall morphology by creating smaller features on top or within the main landform. They play a role in sediment dynamics but on a smaller scale.
3	Subordinate processes	Processes arisen from a different, subsequent morphogenetic system that overlays or converges with the primary one that previously shaped the main landform. When present, these processes act as subordinate contributors to sediment dynamics, producing minor and overimposed features distinguishable over the main landform.
4	Present activity of the main landform	Landforms actively shaped by the primary morphogenetic agent or capable of reactivation under current morphoclimatic conditions are *Active*. Landforms that are no longer actively influenced by the primary morphogenetic agent or cannot be reactivated within the present geomorphic and morphoclimatic setting are *Relict*. For landslides, an additional *Dormant* class is also considered.
5	Past trend of evolution of the geomorphic system	Geomorphic systems in which the overall surface affected by processes has increased, remained stable, or decreased, during the defined time-frame, are respectively classified as *In evolution*, *Stable*, or *In regression*.

diffuse extent that does not allow them to be mapped as individual GEs (i.e. depending on the adopted mapping scale). For this reason, they may not always be identifiable in all the GEs of the same sediment sources/sinks class (i.e. variable 1; Table 1). Hence, secondary and subordinate processes can be assessed by employing a greater survey scale (e.g. 1:2,500) and/or by detecting evidence of their occurrence directly through field surveys. Introducing these definitions (i.e. secondary and subordinate processes) is crucial for effectively acknowledging the presence of complex and polygenetic geomorphic systems (La Licata et al., 2023). This remains applicable even when the limitations of the representation scale hinder detailed mapping. Therefore, different levels of processes identified within a single geomorphic system can be assessed across different spatial scales within the same GE by incorporating geomorphic information as attribute data.

Additionally, superimposed geomorphic systems characterized by main landforms related to distinct and chronologically separated morphogenetic settings, and/or dating back to different morphoclimatic settings, can be mapped at the same scale by overlapping distinct GEs. Particularly, in this latter case, the two overlaid GEs should be part of different sub-databases.

Moreover, the characterization of variables such as *Present activity of the main landform* and *Past trend of evolution of the geomorphic system* can be achieved through a multi-temporal assessment over a defined time-frame (e.g. time series analysis based on geomorphological surveying, photo-interpretative analysis on aerial/satellite images, application of remote sensing techniques, and/or DTMs processing). However, it is noteworthy that the trend of evolution is referred to the present time and it is not considered predictive. Moreover, the past trend of evolution accounts for changes in the affected area due to factors such as vegetation removal or regrowth, even if the perimeter remains unchanged. Anyway, a geomorphic system might be 'in regression' despite the processes still occur in present time or the main landform is reactivable.

In the following sections, we illustrate how this method can be applied at the watershed scale, using the study area as a practical example.

3.2. Acquisition of high-resolution orthophotos

We acquired a series of high-resolution orthophotos covering a 44-years period from national and regional Web Map Services (WMS). National geoportal (http://www.pcn.minambiente.it/mattm/servizio-wms/) provided years 1988, 1996, and 2000. RER geoportal (https://www.geoportale.regione.emilia-romagna.it/catalogo/dati-cartografici/cartografia-di-base/immagini) provided years 1976–1978, 2008, 2011, 2018, 2020 (Red, Green, Blue; RGB), and 2020 (Near Infrared; NIR).

3.3. Assessment of pre-existing georeferenced datasets

We utilized the following datasets provided by regional and national authorities:

- Quaternary deposits, 1:10,000 scale (QD) (SGSS, 2005).
- Italian Landslide Inventory, 1:10,000 scale (IFFI) (APAT, 2007; Trigila et al., 2010).

The QD dataset includes slope and alluvial deposits. It is provided by the Geological, Seismic and Soil Survey (GSSS) of the Emilia-Romagna Region (RER) in shapefile format. Most of the slope deposits in the dataset are classified as 'Slope deposits s.l.' due to their uncertain genesis, lacking clear morphological evidence to relate them to either mass movements or surface runoff.

The IFFI Inventory is the official landslide database of Italy. It is provided by the Italian Institute for Environmental Protection and Research (ISPRA; https://www.progettoiffi.isprambiente.it/cartografia-on-line/; APAT, 2007; Trigila et al., 2010) through a dedicated WMS, according to the EU-INSPIRE-Infrastructure Directive for spatial information (2007/2/CE). It was elaborated by means of the integration of historical landslide data, photointerpretation of aerial images, and field surveys (Trigila et al., 2010). For the RER, the survey scale and the related minimum area for cartographic mapping are respectively 1:10,000 and 1,600 m^2 (Gozza & Pizziolo, 2007; Trigila et al., 2007). Thus, spatially limited landslide deposits below the mapping threshold may not have been mapped. According to Trigila et al. (2007, 2010), falls and topples are grouped into the same class (*i.e.* fall/topples), as are rotational and translational slides (i.e. roto-translational slides). In the study area, most of the landslides are classified as 'complex landslides' (i.e. including both landslides characterized by a combination of movements and rock avalanches). Other landslides are classified as slow mudflows. All the landslides are classified regarding their activity status as *Active* or *Dormant* (APAT, 2007).

Moreover, the RER provided also the regional shapefile datasets of geological and land use data. In particular, the following datasets were acquired:

- Geology (units, limits, and structural elements), 1:25,000 scale (SGSS, 2004a, 2004b, 2004c; Geological Sheet 198 – Bardi, 1:50,000 scale; Servizio Geologico d'Italia, 1999; CARG project);
- Land use 2020, 1:10,000 scale (Regione Emilia-Romagna, 2023).

3.4. Channel network and watershed delineation

We outlined the selected watershed based on a 5 m DTM (Regione Emilia-Romagna, 2019). Firstly, a Gaussian filter of radius 3 was applied to the DTM to remove errors and artifacts. Then, the *Sink Removal* pre-processing tool was applied to deepen drainage routes, using a threshold height of 10 m. Hence, Flow Directions (Wang & Liu, 2006) and Flow Accumulation (Tarboton, 1997) were computed to derive channel network and watershed boundaries.

3.5. DTM-based morphometric analysis

A DTM-based terrain analysis was carried out to characterize the main land-surface features useful for landform identification (Olaya & Conrad, 2009). Particularly, we computed the Analytical Hillshading and some primary morphometric parameters such as Slope, Aspect, Profile Curvature, and Tangential Curvature according to Zevenbergen & Thorne (1987). Moreover, the LS Factor of the Universal Soil Loss Equation (USLE; Wischmeier & Smith, 1978) was computed according to Moore et al. (1991). Furthermore, we performed the GIS-based semi-automatic procedure for landform classification proposed by Weiss (2001), following La Licata et al. (2023). Specifically, this method allows for the classification of landscape features into discrete morphological classes using the Topographic Position Index (TPI; Guisan et al., 1999), achieving a morphological characterization of the study area (De Reu et al., 2013). TPI grids with neighbourhood radius of 80 and 600 m were computed and combined with the slope grid to perform a classification into ten morphological classes: (1) Deeply Incised Streams/Scarps Base, (2) Midslope Drainages, (3) Upland Drainages, (4) Main Valleys, (5) Plains, (6) Open Slopes, (7) Upper Slopes, (8) Local Hills/Ridges in Valleys, (9) Midslope Hills/Ridges on Slopes, (10) Mountain Tops/High Ridges. Finally, we calculated topographic profiles in specific investigation areas (e.g. valley bottom, slope breaks) using the *Profile graph* tool (3D Analyst toolbox, ArcMap) (Zangana et al., 2023).

3.6. Inventory Map: mapping procedure

We produced an Inventory Map (IM) of Geomorphic Entities (GEs) that accounts for the entire range of sediment sources and sinks within the watershed, following Gellis et al. (2016) and Dumitriu et al. (2017). Therefore, GEs were mapped at 1:5,000 scale according to the general methodological framework (Figure 2).

The landform classification map provided an initial representation of the main morphological units. Then, we carried out an extensive photo-interpretative analysis of recent orthophotos and satellite 3D-images, as well as the visual interpretation of Technical Regional Map (1:5,000 scale; Regione Emilia-Romagna, 2020). Particularly, we focused on the identification of morphological and geomorphic features, as well as different vegetation patterns emphasizing the spatial extent of landforms, their genesis, and hydrological elements. Moreover, the hillshade relief map and morphometric parameters were used to interpret the terrain surface in order to investigate the extent and geometric features of landforms (Magliuolo & Valente, 2020). According to Zangana et al. (2023), the hillshade map provided quick information on the terrain features, serving as a background for other layers to better visualize landforms. Furthermore, morphometric parameters such as slope and curvatures, along with topographic cross-sections, provided valuable sources to interpret and digitize steps and breaks in complex slope features, boundaries of landforms, and drainage pathways. Additionally, aspect, flow direction and flow accumulation were used to assess

links between landforms and the drainage system, as well as the direction of processes. Complex and polygenetic geomorphic systems were characterized through detailed field surveys and geomorphological mapping based on a previous work by La Licata et al. (2023). At this mapping stage, our primary focus was directed on assessing the dominant/primary morphogenetic processes to identify and spatially delineate the main landforms using GEs.

Spatial accuracy and consistency of pre-existing datasets were accurately checked and validated adopting a 1:5,000 scale. Subsequently, we made improvements and corrections, such as feature reclassification, redrawing, updating, integration, and mapping of new features. Landslides were mapped primarily using data included in the IFFI Inventory (Figures 3a and 4a). Moreover, we integrated recent landslide events and small-scale landslides below the detection mapping threshold (cfr. Gozza & Pizziolo, 2007; Trigila et al., 2007). Furthermore, landslides whose delimitation included only the accumulation body (Figure 3a) were reshaped to delimit also scarps and crowns (Figure 3b, c, d). According to La Licata et al. (2023), some landslides previously classified as 'complex landslides' in the IFFI were reclassified as 'rock avalanches' (*sensu* Nicoletti & Sorriso-Valvo, 1991). Other complex landslides (*sensu* Cruden & Varnes, 1996) were subdivided and reshaped in order to delimit the different types of movement. Slide-flow landslides were split into a roto-translational movement in the depletion zone and a flow movement in the accumulation zone (Figure 3b, c, d; Figure 4a, b). Flow landslides resulting from a complex style of activity were classified as 'earthflows' (i.e. as to keep the diction in use in literature; Bertolini et al., 2017) and distinguished from 'mudflows' (Figure 3b, c).

Moreover, slope and alluvial deposits were mapped primarily using data included in the QD Inventory (SGSS, 2005). Particularly, they were characterized based on geomorphic process, depositional dynamics, vegetation cover, and extent with respect to the morphological setting. Slope deposits that could not be classified as gravitational or colluvial deposits due to a lack of clear morphological features distinguishable by the techniques applied in this study were classified as 'slope deposits s.l.' (SGSS, 2005).

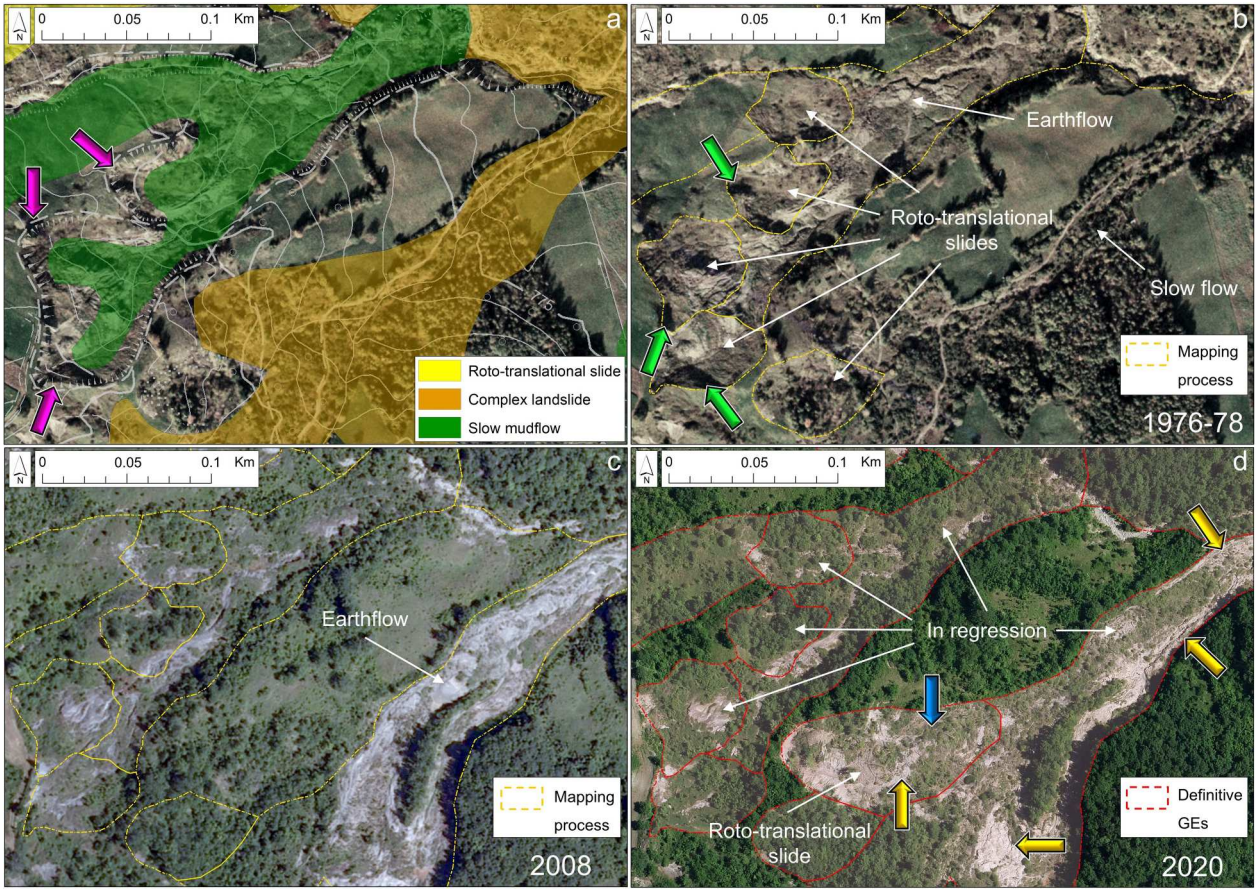

Figure 3. Mapping process starting from the IFFI Inventory (Trigila et al., 2010). (a) Purple arrows highlight some landslide scarps that were not mapped in the IFFI. (b) Morphological characterization of roto-translational slides. Green arrows indicate steep scarps suggesting a sub-vertical movement of the landslide head. Compared to IFFI, the mudflow has been reclassified as 'earthflow'. (c) Evolution of the complex landslide now classified as 'earthflow'. (d) The blue arrow indicates the presence of tensile cracks on landslide body. Yellow arrows indicate evidence of superimposed landforms produced by water erosion processes acting on 'fresh' displaced material (i.e. subordinate process). Definitive Geomorphic Entities (GEs) are contoured in red. The GEs have been classified as *In regression* due to the decrease in surface extent over time mostly caused by increasing vegetation cover.

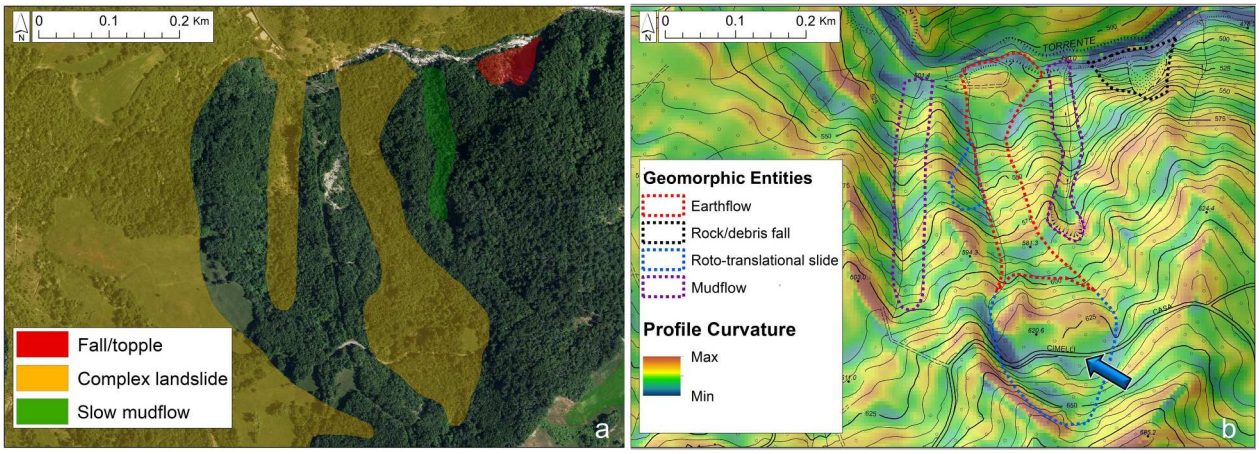

Figure 4. (a) Different landslides as represented in the IFFI Inventory (Trigila et al., 2010). (b) An example of a morphometric parameter used for supporting landform identification and mapping: profile curvature. The blue arrow highlights the concave character of the terrain in correspondence of the surface of rupture, allowing to delimitate the roto-translational source area. These Geomorphic Entities (GEs) are characterized as *Sediment sources/sinks and dynamics* based on the type of movement within the *Landslides* (LD) sub-database.

Additionally, we mapped also landforms and features related to water erosion processes (Figure 5). In particular, we used various criteria to identify rill-interrill erosion features, such as: (i) brightness of the soil due to the erosion of the dark organic topsoil horizon or to the removal of vegetation cover (Figure 5a, b), (ii) specific erosion features visible in the orthophotos and/or satellite images (Figure 5b, c), as well as (iii) the susceptible morphological position revealed by slope map and LS Factor (Maerker et al., 2020). In some cases, we used the NIR Orthophoto 2020 to identify erosion features in areas characterized by shrub and forest revegetation (Figure 5d). Additionally, fluvial erosion features indicating bank retreat and river-related slope erosion were mapped within the fluvial system. Finally, we mapped sediment sources affected by gravity-driven processes separately in cases where specific litho-structural features exert a controlling influence on landform development and sediment dynamics.

3.7. Inventory Map: implementation of the database

According to the general methodological framework (Figure 2), the GEs mapped at 1:5,000 were preliminary subdivided and managed into distinct sub-databases, accounting for artificial groupings that may be useful for the specific case study, as well as for potential overlaps in spatial data. Landslides were managed separately from other slope deposits, rill and interrill erosion features were distinguished from other erosion landforms, and fluvial erosion features were kept separate from fluvial deposits.

Afterwards, we classified the GEs into *Sediment sources/sinks and dynamics* classes (Table 1; Figure 2). In this case study, we partially followed the classification scheme proposed by the Italian Working Group for Geomorphological Mapping (Campobasso et al., 2021), introducing certain modifications to account for specific geomorphic features and the nomenclature commonly used in the reference literature. In particular, landslides were classified based on the type of movement (Cruden & Varnes, 1996; Trigila et al., 2010). Furthermore, we implemented information on *Secondary processes* and *Subordinate processes* by employing a survey scale of 1:2,500 (Table 1; Figure 2). In particular, we focused on the relations between different levels of processes related to different morphogenetic settings, contributing to sediment dynamics on different spatio-temporal scales. Then, an extensive multi-temporal photointerpretation over a 44-years period was carried out at 1:2,500 scale (La Licata et al., 2023) to assess the *Present activity of the main landform*, as well as the *Past trend of evolution of the geomorphic system* over time (Table 1; Figure 2).

Finally, spatial, geometrical, and numerical analyses were carried out on the GEs, using *Sediment sources/sinks and dynamics* as the reference variable.

3.8. WebGIS implementation and visualization

To promote the dissemination of the IM, facilitate evaluation of database completeness and consistency, and enable spatial data visualization at an appropriate scale, we developed a WebGIS application (Bosino et al., 2024; Maerker et al., 2019; Sartirana et al., 2020). Initially, the different GE sub-databases were aggregated and uploaded into a dedicated ArcMap project in order to assemble the Inventory Map (IM). We used the Projected Coordinate System WGS84 – UTM 32N (EPSG: 32632). The IM database was set up to define the properties, symbology, labelling, and visualization criteria of the data layers. The

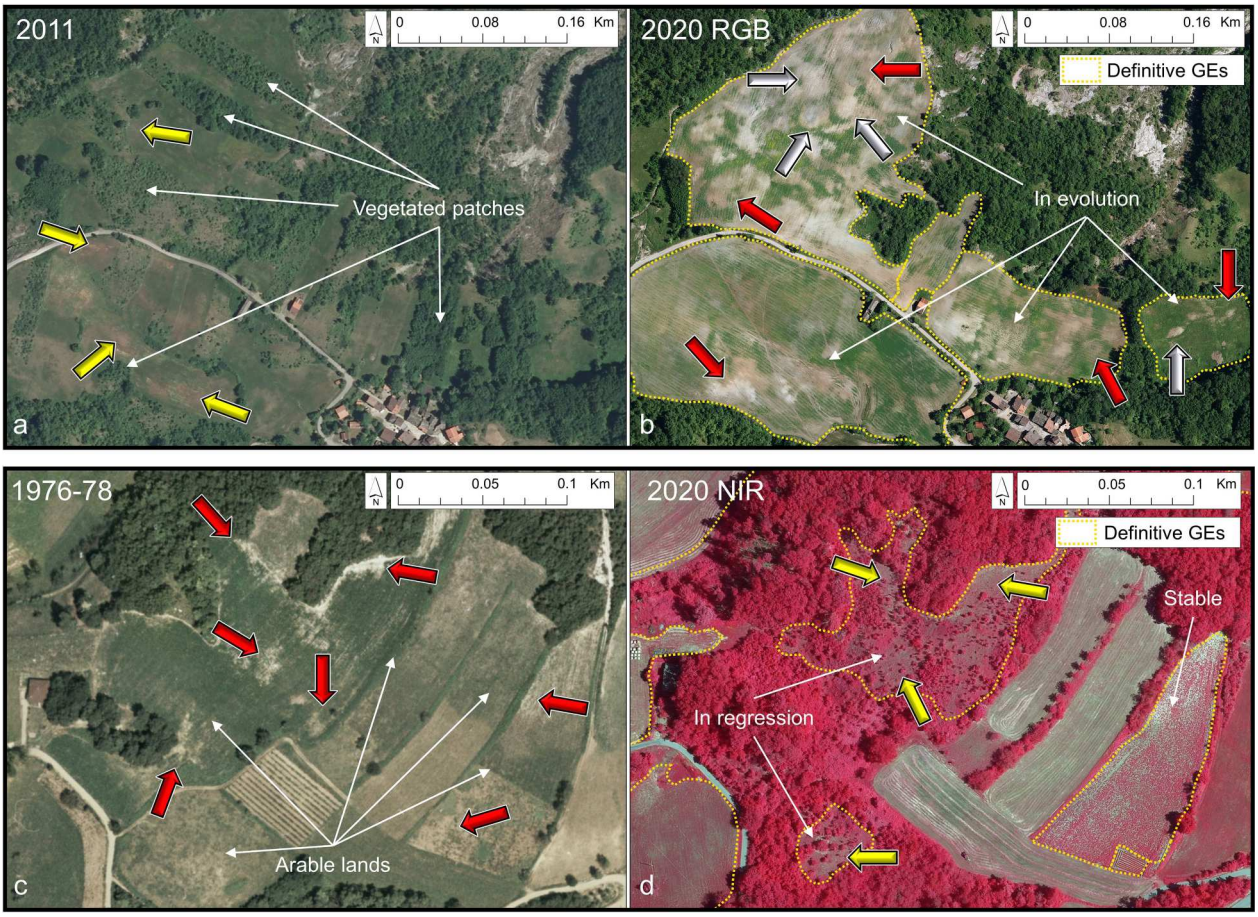

Figure 5. Mapping process of areas affected by rill-interrill erosion. Two different agricultural lands are reported: a-b and c-d. Definitive Geomorphic Entities (GEs) are contoured in yellow (panels *b* and *d*). Panels *a* and *b* show some GEs *In evolution* due to the intensification of tillage and the removal of small vegetated patches protecting soil from water erosion. Panels *c* and *d* show some GEs *In regression* due to partial land abandonment leading to shrub revegetation. Yellow arrows indicate mild rill-interrill erosion. Red arrows indicate severe rill-interrill erosion. White arrows (in panel *b*) indicate superimposed landforms produced by diffuse and small-scale shallow landsliding (*i.e.* subordinate process).

IM data layers were then displayed using a simple colour-based legend based on the *Sediment sources/sinks and dynamics* classification (Figure 2; Table 1). In this way, the GEs were set for displaying and querying up to a maximum scale of 1:5,000. Then, different data layers were added to the project and the structure of the GIS dataframe (i.e. layer order and grouping) was defined. Terrain parameters include *Hillshade Map*, *Slope*, *Aspect*, *Profile Curvature*, *Tangential Curvature*, *LS-Factor*, *Flow Direction*, *Landform Classification*. Additionally, Technical Regional Map, Geology and Land Use data layers (Regione Emilia-Romagna, 2020, 2023; SGSS, 2004a, 2004b, 2004c) were added with a maximum display scale of 1:5,000, 1:25,000 and 1:10,000, respectively. Moreover, the orthophoto dataset was included in the dataframe to facilitate the spatial visualization and interpretation of GE attributes. The ArcMap project was then transferred to the ArcGIS Server and subsequently published through the ArcGIS Online platform. Thus, it can be viewed either through a web browser or Open Geospatial Consortium services (e.g. WMS, WFS) using a client GIS. An Esri© topographic basemap is added to facilitate the localization of the study area in the geographical context. To enhance data accessibility and usability for end-users, we integrated standard WebGIS tools, including coordinate reference system grid overlay, measurement, layer activation/deactivation, zoom, data selection, a geographic search bar, and a searchable database for selective record highlighting.

3.9. Elaboration of the Main Map

The Main Map was created as a complementary product to facilitate access to the WebGIS, providing representative examples to give end-users a clear understanding of its functionality. Additionally, the complete Inventory Map was displayed at a scale of 1:35,000, offering a quick overview of the visual extent and spatial distribution of the GEs. For improving visual representation, GEs within the *Fluvial erosion features* (BE) sub-database were converted and displayed as point features, due to their limited extent. The hillshade relief map was used as base map, along with additional information such as toponyms,

elevation points, contour lines, urban areas, and hydrographic elements derived from the Technical Regional Map.

4. Results

The Inventory Map (IM) includes a total of 2,687 Geomorphic Entities (GEs) covering 4,305 ha, that is, 49% of the total catchment area. The total area increases to 4,640 ha if overlapping GEs are included. The subdivision of the IM into sub-databases and the classification of GEs based on *Sediment sources/sinks and dynamics* are presented in Table 2, along with the main numerical and geometrical outputs from the database analysis. Additional and more detailed results of the statistical analysis can be found in La Licata et al. (2024).

The main result of this study is provided through the WebGIS application, which is freely accessible at the following link: https://unibicocca.maps.arcgis.com/apps/webappviewer/index.html?id=d8bb52f50207475bbe8a34a59bcd456e It allows to assess the extent and spatial distribution of GEs within the IM, enabling end-users to access information stored in the database, alongside additional data layers. Additionally, the Main Map enhances WebGIS accessibility by providing representative examples of querying individual GEs. The Main Map is provided in the Supplementary Materials.

The WebGIS application features a single interface where the IM is displayed and classified based on the *Sediment sources/sinks and dynamics* variable (Figure 2; Table 1), using a simple color-classified symbology. In the top right and left corners of the screen, end-users can access the 'Layer List', where the ArcMap project content is organized under the 'GIS Dataframe' grouping. Automatically active layers include the IM sub-databases (Table 2; with *Fluvial erosion features* (BE) displayed by both points and polygons features), grouped under 'Inventory Map of Geomorphic Entities', as well as the watershed boundary named 'Upper Val d'Arda' and the *Hillshade Map* under 'Terrain parameters'. The Hillshade Map is set to 70% visibility, enabling overlay with other raster layers to enhance topographic features when viewing other terrain parameters. Within 'Terrain parameters', end-users can activate additional layers in the following order: *Slope*, *Aspect*, *Tangential Curvature*, *Profile Curvature*, *LS-Factor*, *Flow Directions*, and *Landform Classification*, all displayed at 100% visibility. Other layers in 'GIS dataframe' include 'Channel network', 'Technical Regional Map 1:5,000', 'Geology 1:25,000 (CARG Project)', and 'Land Use 1:10,000'. Outside of 'GIS Dataframe', end-users can activate WMS orthophotos. Each layer is predisposed for visibility range settings and metadata access. Orthophoto transparency can also be modified. The 'Legend' can be viewed in the top right of the screen, automatically updating with activated/deactivated layers.

Each inventory layer is linked to its attribute table, which includes the following fields: (i) *ID code*, (ii) *Sub-database*, (iii) *Label*, (iv) *Sediment sources/sinks and dynamics*, (v) *Secondary processes*, (vi) *Subordinate processes*, (vii) *Present activity of the main landform*, (viii) *Past trend of evolution of the geomorphic system*, and (ix) *Area (ha)*. By activating 'Filter by

Table 2. Numerical and geometrical output of the Inventory Map database analysis.

Sub-database	Sediment sources/sinks and dynamics	Label	Total Number	Total Number (%)	Area (ha)	Area (%)
Badlands and Gullies		BG	19	0.71	11.90	0.26
	Badlands	BG.1	12	0.45	10.00	0.22
	Isolated gullies	BG.2	7	0.26	1.90	0.04
Rill-Interrill erosion features		RI	1432	53.29	697.41	15.03
	Areas affected by rill-interrill erosion	RI.1	1432	53.29	697.41	15.03
Fluvial erosion features		BE	149	5.55	1.16	0.03
	Retreating banks	BE.1	149	5.55	1.16	0.03
Alluvial deposits		AD	20	0.74	55.32	1.19
	Fluvial terraces	AD.1	16	0.59	44.93	0.97
	Floodplains	AD.2	4	0.15	10.39	0.22
Landslides		LD	927	34.50	3250.95	70.06
	Roto-translational slides	LD.1	519	19.31	584.65	12.60
	Mudflows	LD.2	222	8.26	400.75	8.64
	Earthflows	LD.3	142	5,29	2175.04	46.88
	Block slides	LD.4	25	0.93	78.19	1.68
	Rock/debris falls	LD.5	11	0.41	5.08	0.11
	Debris flows	LD.6	5	0.19	1.04	0.02
	Rock avalanches	LD.7	3	0.11	6.20	0.13
Litho-structural-erosional systems		LR	47	1.75	40.20	0.87
	Rock walls affected by diffuse rock/debris falls	LR.1	47	1.75	40.20	0.87
Slope deposits		SD	93	3.46	582.85	12.56
	Slope deposits s.l.	SD.1	50	1.86	524.99	11.31
	Scree slopes	SD.2	5	0.19	3.78	0.08
	Talus	SD.3	31	1.15	50.03	1.08
	Eluvial deposits	SD.4	7	0.26	4.05	0.09

Note: The total number and the area for each sub-database and *Sediment sources/sinks and dynamics* class is reported. Total Number (%) is referred to the total number of GEs. Area (%) is referred to the total area of GEs.

map extent', only GEs visible within the map view are shown in the attribute table, which updates dynamically with changes in spatial extent or zoom levels. The 'Options' function allows custom query filters to selectively display spatial entities through specific expressions, as well as to display/hide table fields. Selecting a record in the attribute table highlights the respective GE on the map and vice versa, while selecting a GE directly on the map opens a window next to the object, showing information stored in the attribute table (see Main Map).

Additional WebGIS functionalities include a 'Measurement' tool in the top right of the screen to measure area, distance, and position, with selectable units. In the top left, a 'Grid Overlay' tool allows end-users to overlay the coordinate reference grid and adjust the related display settings. Basic functionalities include zooming in/out and resetting to the default extent. The IM has a maximum display threshold of 1:5,000, corresponding to the GEs mapping scale.

The WebGIS facilitates the assessment of information on: (i) process composition within the same GE (i.e. variables 1, 2, and 3; Table 1), (ii) activity and morphodynamics (i.e. variables 4 and 5; Table 1), (iii) the relationships between GEs and terrain parameters, and (iv) the overlapping relationships between GEs. These functionalities make the WebGIS a valuable tool for analysing complex and polygenetic geomorphic systems. For instance, the Main Map is exemplifying the selection of a typical badland (i.e. contoured in light blue), whose information stored in the attribute table appears within a query window. In the study area, *Badlands* (BG.1) (Table 2) have been mapped as geomorphic systems affected by a combination of multiple 'dominant' (i.e. rill-interrill erosion, gully erosion; Figure 6a), 'secondary' (i.e. piping; Figure 6b), and/or 'subordinate' (i.e. landsliding; Figure 6c, e) erosion and depositional processes (Table 1). In the Main Map, tangential curvature shows local flow convergence and divergence, highlighting water flow pathways within drainages such as badland gullies, while slope

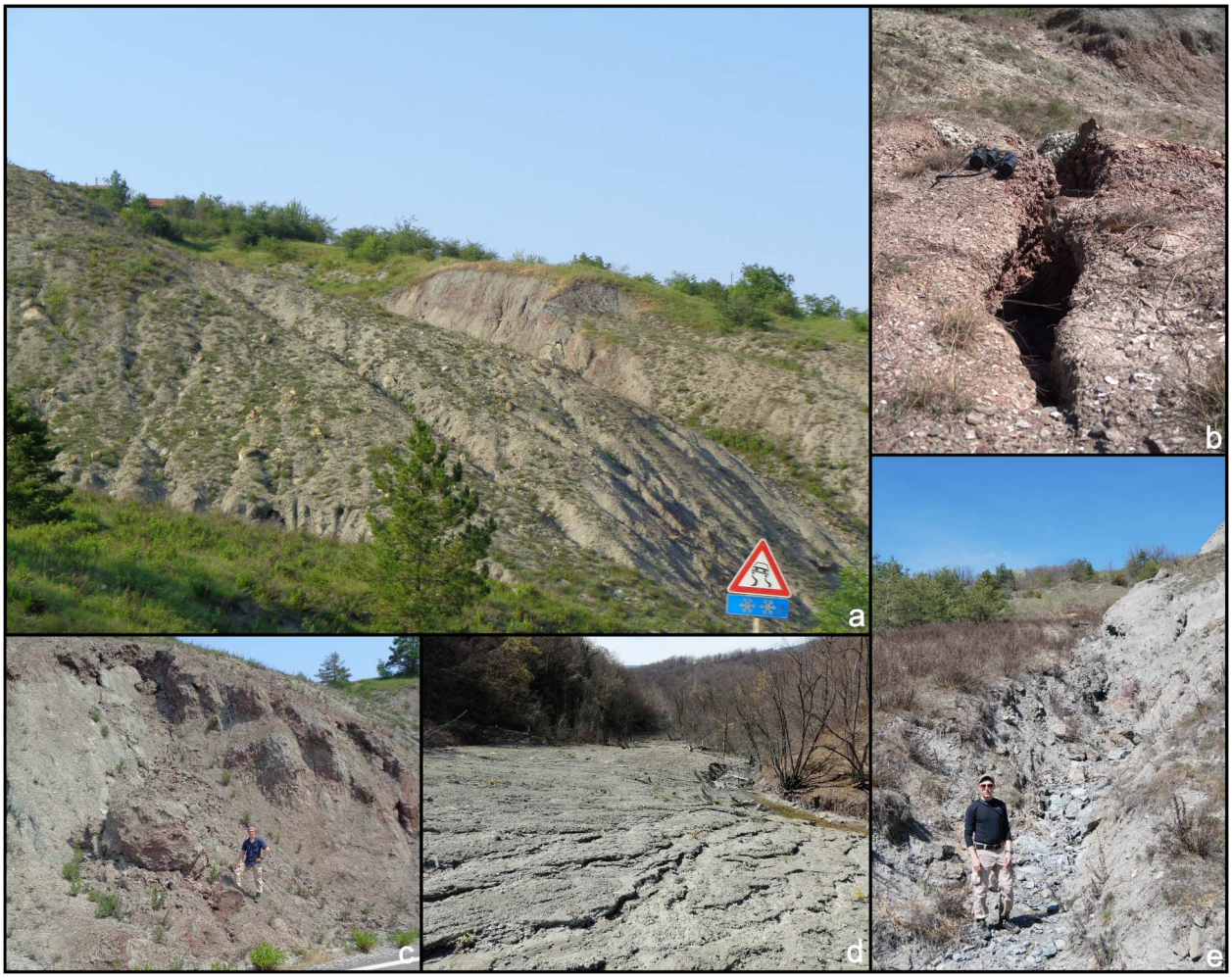

Figure 6. Assessment of geomorphic systems (i.e. hierarchical overlay of processes and related landforms) during field surveys. (a) Evidence of rill-interrill and gully erosion acting as 'dominant/primary morphogenetic processes' on badland development. (b) Evidence of piping acting as 'secondary process' (i.e. related to primary morphogenesis) on a badland system. (c) Rock fall detached from a badland, acting as a 'subordinate process' (i.e. related to a subsequent and overlaying morphogenesis). (d) Rill-interrill erosion features emphasising 'subordinate processes' acting on landslide displaced material. (e) Deposition of coarse-blocky material at the bottom of a gully, as a consequence of diffuse and intermittent small-scale landsliding (i.e. subordinate processes).

map gives insights into overland and subsurface flow velocity and runoff rate (cfr. Wilson & Bishop, 2013). Moreover, the orthophoto time series emphasizes the stable trend of the selected GE (Main Map). Other complex and polygenetic GEs are *Rock walls affected by diffuse rock/debris falls* (LR.1), which are geomorphic systems whose control by litho-structural features influences both landform development and sediment dynamics. In particular, they have been mapped uniformly as GEs affected by diffuse rock/debris falls as 'dominant' process (Table 2), while all of them are further affected by water runoff as 'subordinate' process. Additionally, most of them are affected by debris flows (i.e. 'secondary processes'), mainly occurring along couloir midslope drainages on ribbon-like slopes (La Licata et al., 2023).

Regarding overlapping GEs, *Areas affected by rill-interrill erosion* (RI.1) forming the 'dominant morphogenetic process', on different land uses (e.g. arable lands, meadows), have been considered as independent GEs even when they are imposed on a landslide body stabilized by soil and vegetation. This is especially the case when large landslide bodies have been recognized having an ancient and undefined genesis, thus being preserved in the landscape mostly as morphological features over which human settlements have occurred (Bertolini & Pizziolo, 2008). In this case, RI.1 GEs overlap those of the *Landslide* (LD) sub-database (see Main Map). Another frequent GE overlapping takes place when bank erosion occurs at the landslide toe/flank or within channels intersecting landslide bodies. In this case, *Retreating banks* (BE.1) GEs overlap other GEs within LD (see Main Map).

Conversely, evidence of small-scale surficial water erosion above the 'fresh' landslide displaced material has been considered as a 'subordinate process' of GEs within LD (Figures 3d and 6d; Table 1). Similarly, diffuse and small-scale shallow landsliding (e.g. triggered by prolonged rill-interrill erosion, land use changes, or agricultural practices) has been considered as a 'subordinate process' of RI.1 GEs (Figure 5b; Table 1), rather than being mapped as a landslide process in LD.

5. Discussion

In this paper, we formalized the GIS-based multiscale procedure for sediment sources/sinks mapping introduced by La Licata et al. (2024), illustrating and detailing its conceptual structure and key definitions within a general methodological framework (Figure 2). The novelty of this approach lies in the possibility of representing landscape complexity by using geometrically identifiable polygon objects namely 'Geomorphic Entities' (GEs), which are organized in one or different sub-databases (Figure 7a, b) consisting of structured informative attributes (Table 1). The particular structure of the data and the simplifications introduced with respect to detailed symbol-oriented geomorphological maps – which are often aimed at illustrating the distribution of landforms regardless of the adopted scale and their relevance for application purposes (e.g. Figure 7c, d; Magliuolo & Valente, 2020) – makes our approach more understandable to non-specialist end-users (Griffiths & Abraham, 2008), allowing them to visualize and query complex spatial geomorphological information through the WebGIS. As with other object-oriented approaches (e.g. Buter et al., 2020), using only polygon features (rather than a combination of points, lines, and polygons) facilitates automated GIS analysis, such as the extraction of geometrical and numerical information, improving database analysis (De Jong et al., 2021). However, the results obtained by applying this mapping framework are preliminary and serve as a preparatory work for further elaborations, rather than a final assessment. It is worth noting that our approach efficiently combines both geomorphological and GIS expertise (Rădoane et al., 2011), thus being suitable for GIS-based modelling as well as hazard mapping and zonation (e.g. Gustavsson et al., 2008; van Westen et al., 2003). From this point of view, complex geomorphological information stored in GEs, with a defined spatial distribution and localization, can be used as vector data in (semi-)quantitative modelling procedures involving sediment sources/sinks and dynamics assessment. An example of this kind of application was provided by La Licata et al. (2024), who used structured data stored in IM database to estimate the geomorphic potential of GEs acting as sediment sources, by weighing them based on their process composition and potential contribution to sediment dynamics through a relative scoring system. Afterwards, the weighted GEs were rasterized and integrated with sediment connectivity and sediment transport modelling to assess potential hotspots of sediment sources and related dynamics, as well as to derive 'relative hazard' classes for sediment production and delivery.

Anyway, while our framework is generally applicable across different geographic and morphoclimatic contexts, the specific relationships between processes, landforms, and sediment sources or sinks depend on the geomorphic characteristics of the watershed where it is applied. For instance, in the upper Val d'Arda, slope deposits (SD) and alluvial deposits (AD) (such as scree slopes, talus cones, fluvial terraces, and floodplains; Table 2) are typically considered sediment sinks due to their depositional setting (La Licata et al., 2023). However, these features can also act as sediment sources across various spatial and temporal scales (Gellis et al., 2016), as a function of the degree of sediment (dis)connectivity and the magnitude and frequency of external

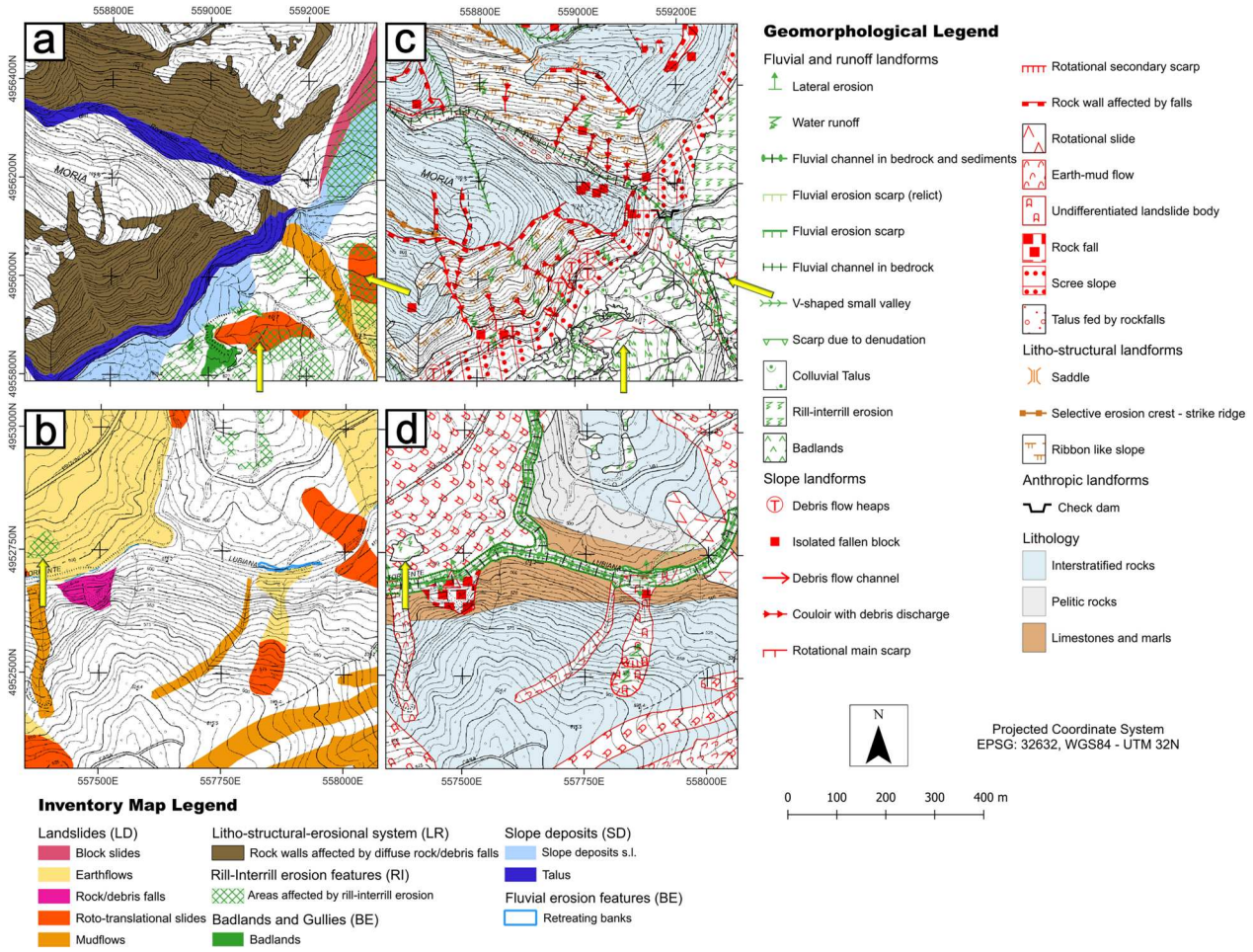

Figure 7. Comparison between the object-oriented 'Geomorphic Entities' mapping approach applied in this study (panels *a* and *b*) and a symbol-oriented geomorphological mapping approach (panels *c* and *d*) (i.e. based on Italian Working Group for Geomorphological Mapping Legend; cfr. Campobasso et al., 2021; modified after La Licata et al., 2023). Two different excerpts are displayed (above and below). The yellow arrows indicate overlapping geomorphic systems.

drivers/forcings (La Licata et al., 2024). Landslides (LD) in this morphoclimatic setting require special attention and are treated separately from other slope deposits. Particularly, large earthflows exemplify the dual role of certain landforms, as they serve as long-term sediment storages due to their persistence and very slow movement rates but can become primary contributors of sediment delivery to the river network when mobility increases (Carlini et al., 2016; Simoni et al., 2013). Consequently, the distinction between sediment 'sources' and 'sinks' is not always clear-cut, as it is a dynamic interplay that varies with temporal scales and geomorphic processes.

In addition, our methodological framework accounts for the problem of representing polygenetic landscapes (Fairbridge, 1968), since different levels of morphogenetic processes overlaying on the same geomorphic system can be easily assessed and characterized by adopting a hierarchical scheme based on different survey scales (Table 1; Figure 2). Thus, several attribute data can be related to the same vector object (Gustavsson et al., 2008; e.g. 'dominant morphogenetic processes' are mapped at 1:5,000 scale defining the GE, while 'subordinate processes' are surveyed at 1:2,500 scale and added as attribute). This makes our approach different from other object-oriented mapping schemes. For instance, in Campobasso et al. (2023) 'focal landforms' can be disaggregated into distinct 'elements' or 'components' to highlight intra-landform complexity, or aggregated to represent 'landform complexes' and 'patterns'. Conversely, our approach assesses geomorphic complexity within the same focal landform as the elementary mapping unit, where a single GE encompasses information on multiple process levels related to different morphogenetic settings, along with information on present activity and its morphodynamic evolution. Furthermore, superimposed morphogenetic systems, chronologically differentiated and forming distinct morphological elements (i.e. palimpsest landscapes; Bauer, 2004; e.g. rill-interrill erosion affecting cultivated areas above wide ancient landslide toe), can be mapped at the same scale using distinct overlaid GEs and stored into distinct information layers (e.g. RI and LD sub-databases; Figure 7a, b). However,

differently from symbol-oriented geomorphological maps, GEs are not suitable to accurately represent landforms through a univocal symbology, from which one can obtain exact information on both present geomorphological and paleo-environmental settings, as well as predict their future development (see Dramis et al., 2011). Thus, since in our approach all the useful geomorphological information related to object-entities is stored in a database, a WebGIS tool is essential to make data accessible to non-GIS experts (Maerker et al., 2019), thereby supporting stakeholders and decision-makers in territorial planning (Karagiozi et al., 2011; Randazzo et al., 2021; Thiebes et al., 2013).

Conversely, a traditional symbol-oriented map is not only useful for outlining the general layout of individual landforms shaped by their morphogenesis, but also for emphasizing the relationships between various landforms, each influenced to different extents by multiple processes (St-Onge, 1981). For instance, Figures 7c and 7d convey a clear and immediate representation of the geomorphological complexity of the area, thanks to a 1:1 relationship between the 'symbol-color' and a particular geomorphological meaning (cfr. Campobasso et al., 2021). Nevertheless, this approach may be less suitable for GIS analysis and modelling due to its genetic-based, scale-dependent symbology, which can lead to challenges when using geospatial data linked by strict topological rules. For instance, in traditional symbol-based geomorphological maps, two overlapping landforms cannot be mapped with polygon symbols (Campobasso et al., 2021). Simplifications are usually adopted to highlight either the primary genetic process (the one responsible for creating the landform being described) or the most recent shaping process that acted on it (Castiglioni, 1982). Thus, in geomorphologically complex areas, the real extent of overlapping landforms might be underestimated (Figure 7c, d). That is, representing process composition of complex overlaying geomorphic systems could be challenging without using a proper symbology differentiated based on both the features to be represented and the scale (i.e. assemblage of point, line, and polygon symbols; Figure 7c, d; Seijmonsbergen, 2013). Hence, depending on the geomorphological legend used, inconsistencies and problems of representation may arise when representing a combination of processes at the same spatial extent without a unified symbology (Rădoane et al., 2011).

6. Conclusion

We provided a GIS-based general methodological framework for assessing, mapping, and interactively visualizing complex and polygenetic landscapes affected by severe land degradation, where different levels of processes overlap and interact on different spatio-temporal scales. By applying our approach in the upper Val d'Arda (Northern Apennines, Italy), we illustrated how complex geomorphological information can be assessed and mapped using polygon objects called 'Geomorphic Entities', allowing to store multiscale information within a hierarchically structured database, including process composition, activity, and morphodynamics. Particularly, our methodological framework addresses many problems typically related to classical symbol-oriented geomorphological maps, making it suitable for both scientific and practical application purposes. However, it should be noted that this method is not designed to replace traditional, symbol-oriented geomorphological mapping, which remains an essential tool for territorial knowledge and characterization. Rather, our approach aims to complement traditional methods, offering a way to manage complex geomorphological data in a form easily implementable in GIS for modelling purposes.

The data are available for interactive consultation in a dedicated WebGIS application. The latter has been implemented as a collection of digital geomorphological information layers, consisting of both raster and vector data, which can be queried and displayed with additional information layers by end-users. Our application allows stakeholders such as local administrations, farmers as well as water and reservoir managers to visualize and use complex information related to geomorphological system dynamics. Further improvements could be addressed towards the implementation of a real decision-support system, supporting decision-makers towards a sustainable watershed management.

Software

We used the Esri© ArcMap software (version 10.3.1; ArcGIS; https://www.esri.com/it) to achieve all the methodological steps aimed at elaborating the Inventory Map (IM), from the acquisition and assessment of pre-existing datasets and digital orthophotos (Web Map Services) to digital mapping and implementation of the database. The Google® Earth 3D Imagery supported the phases related to digital mapping. We used the SAGA GIS software (version 8.1.1; https://saga-gis.sourceforge.io) to achieve the delineation of the channel network and watershed boundary, as well as the DTM-based terrain analysis. Furthermore, the ArcMap 3D Analyst tools were used to elaborate topographic profiles. Statistical analysis on the IM database was performed in Microsoft Excel. The WebGIS implementation was developed through the Esri© ArcGIS Server and

subsequently published through the ArcGIS Online platform.

Acknowledgements

We want to thank the staff of Consorzio di Bonifica di Piacenza (https://www.cbpiacenza.it) for the valuable support during the field surveys. We were also supported by the Belmont ABRESO project (https://www.belmontforum.org) during this research. Finally, the Authors thank the Editor and the three Reviewers for their useful comments and suggestions that helped to improve the manuscript.

Disclosure statement

No potential conflict of interest was reported by the author(s).

Funding

This work was supported by: PNRR Project 'GeoSciences IR' M4 - C 2 - L.I.3.1. (European Commission, Next Generation EU CUP: I53C22000800006); PRIN project 2022C2XPK7 funded by the Italian Ministry of University and Research, entitled: 'Full cOveRage, Multi-scAle and multi-sensor geomorphological map: a practical tool for TerrItOrial plaNning - FORMATION'; Earth and Environmental Sciences PhD-PON program of University of Pavia (Research & Innovation, 2014-2020, Education and research for recovery - REACT-EU) [DOT1322534-4]; RTDA-PON program of University of Milano-Bicocca (Research & Innovation 2014-2020, Education and research for recovery - REACT-EU) [C6-G-32370-3].

Data availability statement

The data that support the findings of this study are made freely available for visualization, consultation, and querying at the following site: https://unibicocca.maps.arcgis.com/apps/webappviewer/index.html?id=d8bb52f50207475bbe8a34a59bcd456e The complete dataset is deposited with the corresponding author, [M.L.] and will be made available upon reasonable request.

ORCID

Manuel La Licata http://orcid.org/0000-0001-9106-6408
Alberto Bosino http://orcid.org/0000-0001-5032-8467

References

APAT - Agenzia per la Protezione dell'Ambiente e per i Servizi Tecnici. (2007). *Rapporto sulle frane in Italia. Il Progetto IFFI – Metodologia, risultati e rapporti regionali*. Rapporti APAT 78/2007.

Bartelletti, C., Giannecchini, R., D'Amato Avanzi, G., Galanti, Y., & Mazzali, A. (2017). The influence of geological–morphological and land use settings on shallow landslides in the Pogliaschina T. basin (northern Apennines, Italy). *Journal of Maps*, *13*(2), 142–152. https://doi.org/10.1080/17445647.2017.1279082

Bauer, B. O. (2004). Geomorphology. In A. S. Goudie (Ed.), *Encyclopedia of geomorphology* (Vol. 1, pp. 428–435). Routledge Ltd, Taylor & Francis Group.

Bertolini, G., Corsini, A., & Tellini, C. (2017). Fingerprints of large-scale landslides in the landscape of the Emilia Apennines. In M. Soldati & M. Marchetti (Eds.), *Landscapes and Landforms of Italy. World geomorphological landscapes* (pp. 215–224). Springer. https://doi.org/10.1007/978-3-319-26194-2_18

Bertolini, G., & Pizziolo, M. (2008). Risk assessment strategies for the reactivation of earth flows in the Northern Apennines (Italy). *Engineering Geology*, *102*(3–4), 178–192. https://doi.org/10.1016/j.enggeo.2008.03.017

Bishop, M. P., James, L. A., Shroder, J. F., & Walsh, S. J. (2012). Geospatial technologies and digital geomorphological mapping: Concepts, issues and research. *Geomorphology*, *137*(1), 5–26. https://doi.org/10.1016/j.geomorph.2011.06.027

Bishop, M. P., & Shroder, J. F. (Eds.). (2004). *Geographic information science and mountain geomorphology*. Springer-Praxis.

Bollati, I. M., Cavalli, M., Masseroli, A., Viani, C., Moraschina, F., & Pelfini, M. (2024). Thematic mapping for sediment cascade analysis in small mountain catchments – The case of the Buscagna valley (Lepontine Alps). *Geomorphology*, *446*, 109001. https://doi.org/10.1016/J.GEOMORPH.2023.109001

Bosino, A., Mandarino, A., De Amicis, M., Cazzini, F. F., El Khair, D. A., & Flores, P. (2024). Assessment of piping-sinkhole development in a fluvial-terrace scarp retreat environment: A multi-temporal analysis on the lower Ticino River (Italy). *Geomorphology*, *450*, 109082. https://doi.org/10.1016/j.geomorph.2024.109082

Bosino, A., Szatten, D. A., Omran, A., Crema, S., Crozi, M., Becker, R., Bettoni, M., Schillaci, C., & Maerker, M. (2022). Assessment of suspended sediment dynamics in a small ungauged badland catchment in the Northern Apennines (Italy) using an in-situ laser diffraction method. *Catena*, *209*, 105796. https://doi.org/10.1016/j.catena.2021.105796

Bufalini, M., Materazzi, M., De Amicis, M., & Pambianchi, G. (2021). From traditional to modern 'full coverage' geomorphological mapping: a study case in the Chienti river basin (Marche region, central Italy). *Journal of Maps*, *17*(3), 17–28. https://doi.org/10.1080/17445647.2021.1904020

Buter, A., Spitzer, A., Comiti, F., & Heckmann, T. (2020). Geomorphology of the Sulden River basin (Italian Alps) with a focus on sediment connectivity. *Journal of Maps*, *16*(2), 890–901. https://10.108017445647.2020.1841036

Campobasso, C., Carton, A., Chelli, A., D' Orefice, M., Dramis, F., Graciotti, R., Guida, D., Pambianchi, G., Peduto, F., & Pellegrini, L. (2021). *Aggiornamento ed integrazioni delle linee guida della Carta Geomorfologica d'Italia alla scala 1:50000 e banca dati geomorfologica. Carta Geomorfologica d'Italia alla scala 1:50000. Fascicolo I, Versione 2.0. Quaderni del Servizio Geologico Nazionale, Ser. III, 13*. Istituto Poligrafico e Zecca dello Stato.

Campobasso, C., Pambianchi, G., Peduto, F., Cestari, A., Chelli, A., Congi, M. P., D'Orefice, M., De Amicis, M., Dramis, F., Graciotti, R., Guida, D., Palmieri, V., Pellegrini, L., Valiante, M., & Ventura, R. (2023). *Proposta di un nuovo modello di cartografia geomorfologica a indirizzo applicativo. Carta Geomorfologica d'Italia alla scala 1:50000. Fascicolo II, Versione 1.0. Quaderni del Servizio Geologico Nazionale, Ser. III, 13*. Istituto Poligrafico e Zecca dello Stato.

Carlini, M., Chelli, A., Vescovi, P., Artoni, A., Clemenzi, L., Tellini, C., & Torelli, L. (2016). Tectonic control on the

development and distribution of large landslides in the Northern Apennines (Italy). *Geomorphology*, *253*, 425–437. https://doi.org/10.1016/j.geomorph.2015.10.028

Castiglioni, G. B. (1982). La cartografia geomorfologica tra ricerca di base e ricerca applicata. *Bollettino della Società Geografica Italiana*, *11*, 609–632.

Cho, S. J., Karwan, D. L., Skalak, K., Pizzuto, J., & Huffman, M. E. (2023). Sediment sources and connectivity linked to hydrologic pathways and geomorphic processes: a conceptual model to specify sediment sources and pathways through space and time. *Frontiers in Water*, *5*, 1241622. https://doi.org/10.3389/frwa.2023.1241622

Cruden, D. M., & Varnes, D. J. (1996). Landslide types and processes. In A. K. Turner & R. L. Schuster (Eds.), *Landslide investigation and mitigation. Transportation research board* (pp. 36–75). US National Research Council. Special Report 247, Chapter 3.

De Jong, M. G. G., Sterk, H. P., Shinneman, S., & Seijmonsbergen, A. C. (2021). Hierarchical geomorphological mapping in mountainous areas. *Journal of Maps*, *17*(2), 214–224. https://doi.org/10.1080/17445647.2021.1897047

De Reu, J., Bourgeois, J., Bats, M., Zwertvaegher, A., Gelorini, V., De Smedt, P., Chu, W., Antrop, M., De Maeyer, P., Finke, P., Van Meirvenne, M., Verniers, J., & Crombé, P. (2013). Application of the topographic position index to heterogeneous landscapes. *Geomorphology*, *186*, 39–49. https://doi.org/10.1016/j.geomorph.2012.12.015

Dramis, F., Guida, D., & Cestari, A. (2011). Nature and aims of geomorphological mapping. In M. J. Smith, P. Paron, & J. S. Griffiths (Eds.), *Geomorphological mapping, methods and applications. Developments in earth surface processes* (Vol. *15*, pp. 39–73). https://doi.org/10.1016/B978-0-444-53446-0.00003-3

Dumitriu, D., Rădoane, M., & Rădoane, N. (2017). Sediment Sources and Delivery. In M. Rădoane & A. Vespremeanu-Stroe (Eds.), *Landform Dynamics and Evolution in Romania* (pp. 629–654). Springer Geography, Springer Cham. https://doi.org/10.1007/978-3-319-32589-7_27.

Fairbridge, R. W. (1968). *The Encyclopedia of geomorphology*. Encyclopedia of earth sciences series. Dowden, Hutchinson & Ross, Inc.

Gao, P., Cooper, J. R., & Wainwright, J. (2019). Toward understanding complexity of sediment dynamics in geomorphic systems. *Geomorphology*, *330*, 129–132. https://doi.org/10.1016/J.GEOMORPH.2019.01.018

Gellis, A., Fitzpatrick, F., & Schubauer-Berigan, J. (2016). *A manual to identify sources of fluvial sediment*. Office of Research and Development, National Risk Management Research Laboratory, Land Remediation and Pollution Control Division. United States Environmental Protection Agency – EPA/600/R-16/210.

Gozza, G., & Pizziolo, M. (2007). Analisi del dissesto da frana in Emilia-Romagna. In Agenzia per la Protezione dell'Ambiente e per i Servizi Tecnici (Ed.), *Rapporto sulle frane in Italia. Il Progetto IFFI – Metodologia, risultati e rapporti regionali* (pp. 329–353). Rapporti APAT 78/2007.

Griffiths, J. S., & Abraham, J. K. (2008). Factors affecting the use of applied geomorphology maps to communicate with different end-users. *Journal of Maps*, *4*(1), 201–210. https://doi.org/10.4113/jom.2008.89

Guisan, A., Weiss, S. B., & Weiss, A. D. (1999). GLM versus CCA spatial modeling of plant species distribution. *Plant Ecology*, *143*(1), 107–122. https://doi.org/10.1023/A:1009841519580

Gustavsson, M., Kolstrup, E., & Seijmonsbergen, A. C. (2006). A new symbol-and-GIS based detailed geomorphological mapping system: Renewal of a scientific discipline for understanding landscape development. *Geomorphology*, *77*(1–2), 90–111. https://doi.org/10.1016/J.GEOMORPH.2006.01.026

Gustavsson, M., Seijmonsbergen, A. C., & Kolstrup, E. (2008). Structure and contents of a new geomorphological GIS database linked to a geomorphological map — With an example from Liden, central Sweden. *Geomorphology*, *95*(3–4), 335–349. https://doi.org/10.1016/j.geomorph.2007.06.014

IUSS Working Group WRB. (2015). *World reference base for soil resources 2014, update 2015. International soil classification system for naming soils and creating legends for soil maps*. World Soil Resources Reports No. 106. FAO.

James, L. A., Walsh, S. J., & Bishop, M. P. (2012). Geospatial technologies and geomorphological mapping. *Geomorphology*, *137*(1), 1–4. https://doi.org/10.1016/j.geomorph.2011.06.002

Karagiozi, E., Fountoulis, I., Konstantinidis, A., Andreadakis, E., & Ntouros, K. (2011). *Flood hazard assessment based on geomorphological analysis with GIS tools - The case of Laconia (Peloponnesus, Greece)*. Proceedings, Symposium GIS Ostrava.

Kottek, M., Grieser, J., Beck, C., Rudolf, B., & Rubel, F. (2006). World map of the Köppen-Geiger climate classification updated. *Meteorologische Zeitschrift*, *15*(3), 259–263. https://doi.org/10.1127/0941-2948/2006/0130

La Licata, M., Bosino, A., Bettoni, M., & Maerker, M. (2023). Assessing landscape features and geomorphic processes influencing sediment dynamics in a geomorphologically highly active Mediterranean agroecosystem: The upper Val d'Arda case study (Northern Apennines, Italy). *Geomorphology*, *433*, 108724. https://doi.org/10.1016/j.geomorph.2023.108724

La Licata, M., Bosino, A., Sadeghi, S. H., De Amicis, M., Mandarino, A., Terret, A., & Maerker, M. (2024). HOTSED: A new integrated model for assessing potential hotspots of sediment sources and related sediment dynamics at watershed scale. *International Soil and Water Conservation Research*, https://doi.org/10.1016/j.iswcr.2024.06.002

Maerker, M., Bosino, A., Scopesi, C., Giordani, P., Firpo, M., & Rellini, I. (2020). Assessment of calanchi and rill-interrill erosion susceptibility in northern Liguria, Italy: A case study using a probabilistic modelling framework. *Geoderma*, *371*, 114367. https://doi.org/10.1016/j.geoderma.2020.114367

Maerker, M., Moretti, S., & Rodolfi, G. (2001). Assessment of water erosion processes and dynamics in semi-arid regions of southern Africa (KwaZulu/Natal RSA, and Swaziland) using the Erosion Response Units Concept (ERU). *Geogr. Fis. Dinam. Quat*, *24*, 71–83.

Maerker, M., Schillaci, C., Melis, R. T., Kropáček, J., Bosino, A., Vilímek, V., Hochschild, V., Sommer, C., Altamura, F., & Mussi, M. (2019). Geomorphological processes, forms and features in the surroundings of the Melka Kunture Palaeolithic site, Ethiopia. *Journal of Maps*, *15*(2), 797–806. https://doi.org/10.1080/17445647.2019.1669497

Magliuolo, P., & Valente, A. (2020). GIS-Based Geomorphological Map of the Calore River Floodplain Near Benevento (Southern Italy) Overflooded by the 15th October 2015 Event. *Water*, *12*(1), 148. https://doi.org/10.3390/w12010148

Marroni, M., Molli, G., Ottria, G., & Pandolfi, L. (2001). Tectono-sedimentary evolution of the External Liguride units (Northern Apennines, Italy): Insights in the pre-collisional history of a fossil ocean-continent transition zone. *Geodinamica Acta*, *14*(5), 307–320. https://doi.org/10.1080/09853111.2001.11432449

Martini, A., & Zanzucchi, G. (2000). *Note Illustrative della Carta Geologica d'Italia alla scala 1:50000, Foglio 198 - Bardi*. Servizio Geologico d'Italia.

Minár, J., Drăguț, L., Evans, I. S., Feciskanin, R., Gallay, M., Jenčo, M., & Popov, A. (2024). Physical geomorphometry for elementary land surface segmentation and digital geomorphological mapping. *Earth-Science Reviews*, *248*, 104631. https://doi.org/10.1016/J.EARSCIREV.2023.104631

Moore, I. D., Grayson, R. B., & Ladson, A. R. (1991). Digital terrain modelling: a review of hydrological, geomorphological, and biological applications. *Hydrological Processes*, *5*(1), 3–30. https://doi.org/10.1002/hyp.3360050103

Najafi, S., Sadeghi, S. H., & Heckmann, T. (2021). Analysis of sediment accessibility and availability concepts based on sediment connectivity throughout a watershed. *Land Degradation & Development*, *32*(10), 3023–3044. https://doi.org/10.1002/ldr.3964

Nicoletti, P. G., & Sorriso-Valvo, M. (1991). Geomorphic controls of the shape and mobility of rock avalanches. *Geological Society of America Bulletin*, *103*(10), 1365–1373. https://doi.org/10.1130/0016-7606(1991)103%3C1365:GCOTSA%3E2.3.CO;2

Olaya, V., & Conrad, O. (2009). Geomorphometry in SAGA. In T. Hengl & H. I. Reuter (Eds.), *Geomorphometry, concepts, software, applications. Developments in soil science* (Vol. 33, pp. 293–308). Elsevier Ltd. https://doi.org/10.1016/S0166-2481(08)00012-3

Panizza, M. (1972). Schema di legenda per carte geomorfologiche di dettaglio. *Bollettino della Società Geologica Italiana*, *91*(2), 207–237.

Patro, E. R., De Michele, C., Granata, G., & Biagini, C. (2022). Assessment of current reservoir sedimentation rate and storage capacity loss: An Italian overview. *Journal of Environmental Management*, *320*, 115826. https://doi.org/10.1016/j.jenvman.2022.115826

Rădoane, M., Cristea, I., & Rădoane, N. (2011). Geomorphological mapping. *Evolution and Trends. Revista de Geomorfologie*, *13*, 19–39.

Randazzo, G., Italiano, F., Micallef, A., Tomasello, A., Cassetti, F. P., Zammit, A., D'amico, S., Saliba, O., Cascio, M., Cavallaro, F., Crupi, A., Fontana, M., Gregorio, F., Lanza, S., Colica, E., & Muzirafuti, A. (2021). WebGIS implementation for dynamic mapping and visualization of coastal geospatial data: A case study of BESS project. *Applied Sciences*, *11*(17), 8233. https://doi.org/10.3390/app11178233

Regione Emilia-Romagna, 1994. I suoli dell'Emilia-Romagna. Note Illustrative. Servizio Cartografico – Ufficio Pedologico, pp. 383.

Regione Emilia-Romagna. (2019). *Modello Digitale del Terreno 5x5, Edizione 2014. Archivio Cartografico*. Geoportale Regione Emilia-Romagna. https://www.geoportale.regione.emilia-romagna.it/catalogo/dati-cartografici/altimetria/layer-2

Regione Emilia-Romagna. (2020). *DBTR – Carta Tecnica Regionale 1:5000. Settore innovazione digitale, dati, tecnologia e polo archivistico*. Geoportale Regione Emilia-Romagna. https://www.geoportale.regione.emilia-romagna.it/catalogo/dati-cartografici/cartografia-di-base/cartografia-tecnica/layer-1

Regione Emilia-Romagna. (2023). *Coperture vettoriali uso del suolo di dettaglio 2020 – Edizione 2023. Settore innovazione digitale, dati, tecnologia e polo archivistico*. Geoportale Regione Emilia-Romagna. https://geoportale.regione.emilia-romagna.it/catalogo/dati-cartografici/pianificazione-e-catasto/uso-del-suolo/layer-14

Renschler, C. S., & Harbor, J. (2002). Soil erosion assessment tools from point to regional scales—the role of geomorphologists in land management research and implementation. *Geomorphology*, *47*(2–4), 189–209. https://doi.org/10.1016/S0169-555X(02)00082-X

Sadeghi, S. H., Najafi, S., Bakhtiari, A. R., & Abdi, P. (2014). Ascribing soil erosion types for sediment yield using composite fingerprinting technique. *Hydrological Sciences Journal*, *59*(9), 1753–1762. https://doi.org/10.1080/02626667.2014.940955

Sartirana, D., Rotiroti, M., Zanotti, C., Bonomi, T., Fumagalli, L., & De Amicis, M. (2020). A 3D geodatabase for urban underground infrastructures: implementation and application to groundwater management in Milan metropolitan area. *ISPRS International Journal of Geo-Information*, *9*(10), 609. https://doi.org/10.3390/ijgi9100609

Seijmonsbergen, A. C. (2013). The modern geomorphological map. In J. Shroder (Editor in Chief), A. D. Switzer, & D. M. Kennedy (Eds.), *Treatise on geomorphology*, vol. 14, Methods in Geomorphology (pp. 35–52). Academic Press. http://doi.org/10.1016/B978-0-12-374739-6.00371-7

Servizio Geologico d'Italia. (1999). Carta Geologica d'Italia alla scala 1:50000, Foglio 198 - Bardi. Istituto Poligrafico e Zecca dello Stato, Roma.

SGSS - Servizio Geologico, Sismico e dei Suoli. (2004a). Carta geologica, 1:25.000 – Elementi strutturali – 50k. Regione Emilia-Romagna, Settore Difesa del Territorio. Geoportale Regione Emilia-Romagna. https://geoportale.regione.emilia-romagna.it/catalogo/dati-cartografici/informazioni-geoscientifiche/geologia/carta-geologica-1-25.000/layer-19

SGSS - Servizio Geologico, Sismico e dei Suoli (2004b). Carta geologica, 1:25.000 – Formazioni geologiche – 50k. Regione Emilia-Romagna, Settore Difesa del Territorio. Geoportale Regione Emilia-Romagna. https://geoportale.regione.emilia-romagna.it/catalogo/dati-cartografici/informazioni-geoscientifiche/geologia/carta-geologica-1-25.000/layer

SGSS - Servizio Geologico, Sismico e dei Suoli (2004c). Carta geologica, 1:25.000 – Limiti di unità cartografabili geologiche – 50k. Regione Emilia-Romagna, Settore Difesa del Territorio. Geoportale Regione Emilia-Romagna. https://geoportale.regione.emilia-romagna.it/catalogo/dati-cartografici/informazioni-geoscientifiche/geologia/carta-geologica-1-25.000/layer-21

SGSS - Servizio Geologico, Sismico e dei Suoli. (2005). Banca dati geologica, 1:10.000 – Frane, depositi di versante e depositi alluvionali – 10k. Regione Emilia-Romagna, Settore Difesa del Territorio. Geoportale Regione Emilia-Romagna. https://geoportale.regione.emilia-romagna.it/catalogo/dati-cartografici/informazioni-geoscientifiche/geologia/banca-dati-geologica-1-10.000layer-4

Simoni, A., Ponza, A., Picotti, V., Berti, M., & Dinelli, E. (2013). Earthflow sediment production and Holocene sediment record in a large Apennine catchment. *Geomorphology*, *188*, 42–53. https://doi.org/10.1016/j.geomorph.2012.12.006

St-Onge, D. A. (1981). Theories, paradigms, mapping and geomorphology. *Canadian Geographies / Géographies*

canadiennes, *25*(4), 307–315. https://doi.org/10.1111/j.1541-0064.1981.tb01335.x

Tarboton, D. G. (1997). A new method for the determination of flow directions and upslope areas in grid digital elevation models. *Water Resources Research*, *33*(2), 309–319. https://doi.org/10.1029/96WR03137

Theler, D., & Reynard, E. (2008). Mapping Sediment Transfer Processes Using GIS Applications. 6th ICA Mountain Cartography Workshop Mountain Mapping and Visualisation, 227-234.

Theler, D., Reynard, E., & Bardou, E. (2008). Assessing sediment dynamics from geomorphological maps: Bruchi torrential system, Swiss alps. *Journal of Maps*, *4*(1), 277–289. https://doi.org/10.4113/jom.2008.1013

Theler, D., Reynard, E., Lambiel, C., & Bardou, E. (2010). The contribution of geomorphological mapping to sediment transfer evaluation in small alpine catchments. *Geomorphology*, *124*(3–4), 113–123. https://doi.org/10.1016/j.geomorph.2010.03.006

Thiebes, B., Bell, R., Glade, T., Jäger, S., Anderson, M., & Holcombe, L. (2013). A WebGIS decision-support system for slope stability based on limit-equilibrium modelling. *Engineering Geology*, *158*, 109–118. https://doi.org/10.1016/j.enggeo.2013.03.004

Trigila, A., Iadanza, C., & Rischia, I. (2007). Metodologia di lavoro e struttura della banca dati. In Agenzia per la Protezione dell'Ambiente e per i Servizi Tecnici (Ed.), *Rapporto sulle frane in Italia. Il Progetto IFFI – Metodologia, risultati e rapporti regionali* (pp. 3–30). Rapporti APAT 78/2007.

Trigila, A., Iadanza, C., & Spizzichino, D. (2010). Quality assessment of the Italian Landslide Inventory using GIS processing. *Landslides*, *7*(4), 455–470. https://doi.org/10.1007/s10346-010-0213-0

van Westen, C. J., Rengers, N., & Soeters, R. (2003). Use of geomorphological information in indirect landslide susceptibility assessment. *Natural Hazards*, *30*(3), 399–419. https://doi.org/10.1023/B:NHAZ.0000007097.42735.9e

Veenendaal, B., Brovelli, M. A., & Li, S. (2017). Review of web mapping: Eras, trends and directions. *ISPRS International Journal of Geo-Information*, *6*(10), 317. https://doi.org/10.3390/ijgi6100317

Wang, L., & Liu, H. (2006). An efficient method for identifying and filling surface depressions in digital elevation models for hydrologic analysis and modelling. *International Journal of Geographical Information Science*, *20*(2), 193–213. https://doi.org/10.1080/13658810500433453

Weiss, A. D. (2001). Topographic Position And Landforms Analysis. Poster Presentation, ESRI Users Conference, San Diego, CA.

Wilson, J. P., & Bishop, M. P. (2013). 3.7 Geomorphometry. *Treatise on geomorphology*, 3, 162–186. http://doi.org/10.1016/B978-0-12-374739-6.00049-X

Wischmeier, W. H., & Smith, D. D. (1978). *Predicting rainfall erosion losses - A guide to conservation planning. Agriculture Handbook No. 537*. US Department of Agriculture.

Zangana, I., Otto, J. C., Mäusbacher, R., & Schrott, L. (2023). Efficient geomorphological mapping based on geographic information systems and remote sensing data: an example from Jena, Germany. *Journal of Maps*, *19*(1), 2172468. https://doi.org/10.1080/17445647.2023.2172468

Zevenbergen, L. W., & Thorne, C. R. (1987). Quantitative analysis of land surface topography. *Earth Surface Processes and Landforms*, *12*(1), 47–56. https://doi.org/10.1002/esp.3290120107